

Supporting Information

Dual Electrocatalytic Heterostructures for Efficient Immobilization and Conversion of Polysulfides in Li-S Batteries

Menghua Yang,^a Xuewei Wang,^a Jinfeng Wu,^a Yue Tian,^a Xingyu Huang,^a Ping Liu,^a Xianyang Li,^b Xinru Li,^b Xiaoyan Liu,^a Hexing Li*^a*

^aThe Education Ministry Key Lab of Resource Chemistry, Joint International Research Laboratory of Resource Chemistry, Ministry of Education, Shanghai Key Laboratory of Rare Earth Functional Materials, College of Chemistry and Materials Science, Shanghai Normal University, Shanghai 200234, China

^bDepartment of Chemical and Biomolecular Engineering
University of California, Los Angeles
Los Angeles, CA 90095, United States

*corresponding authors:

Xiaoyan Liu, Email: xyliu@shnu.edu.cn,
Hexing Li, Email: hexing-li@shnu.edu.cn

Table S1 The specific surface areas of different samples.

Sample	Specific surface area ($\text{m}^2 \text{ g}^{-1}$)
Co-Zn/Zn-C-700	13
Co-Zn/Zn-C-800	131
Co-Zn/Zn-C-900	676
Co-Zn/Zn-C-800-1	137
Co-Zn/Zn-C-800-3	76

Table S2 The real contents of Zn and Co in different samples achieved by ICP.

Sample	Co (wt%)	Zn (wt%)
Co-Zn/Zn-C-700	0.99	23.6
Co-Zn/Zn-C-800	1.76	14.2
Co-Zn/Zn-C-900	2.79	2.08

Table S3 Comparison of electrochemical performances among Co-Zn/Zn-C-800/S electrode and the literature reported sulfur cathodes.¹⁻¹¹

Sample	Rate	Cycle number	Reversible capacity (mAh g ⁻¹)	Ref.
CoP@HPCN/S	0.2 C	300	630	1
S/PCMSs	0.5 C	700	489	2
CNT@TiO _{2-x} -S	1 C	500	590	3
S@TiO ₂ @HCNBs	0.5 C	600	508	4
CF/FeP@C@S	1 C	200	500	5
CNT/CdS-QDs/S	0.5 C	150	820.6	6
CGPE	1 C	200	580	7
S-SAV@NG	0.5 C	400	551	8
B/2D MOF-Co	1 C	600	450	9
Sph-Ox-S	0.2 C	300	700	10
V ₂ O ₅ -S-CNG	0.5 C	150	713.3	11
Co-Zn/Zn-C-800/S	1 C	500	590	This work

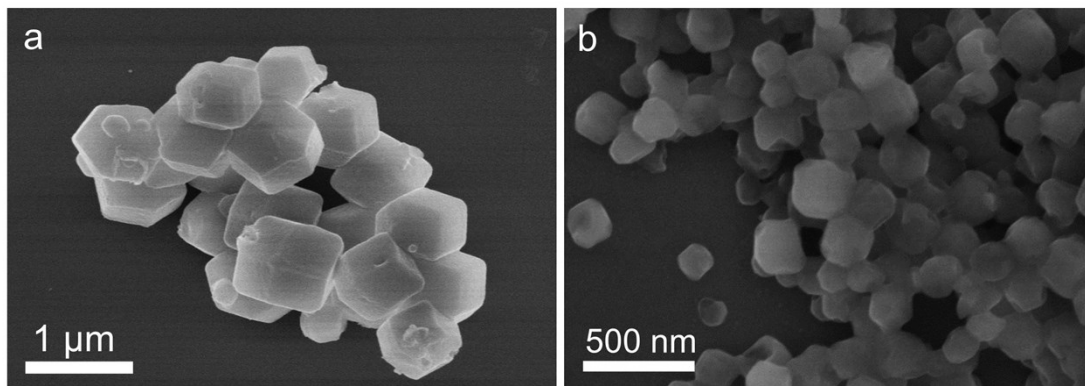


Fig. S1 SEM images of (a) Zn/Co-ZIF and (b) Zn/Co-ZIF@PZS.

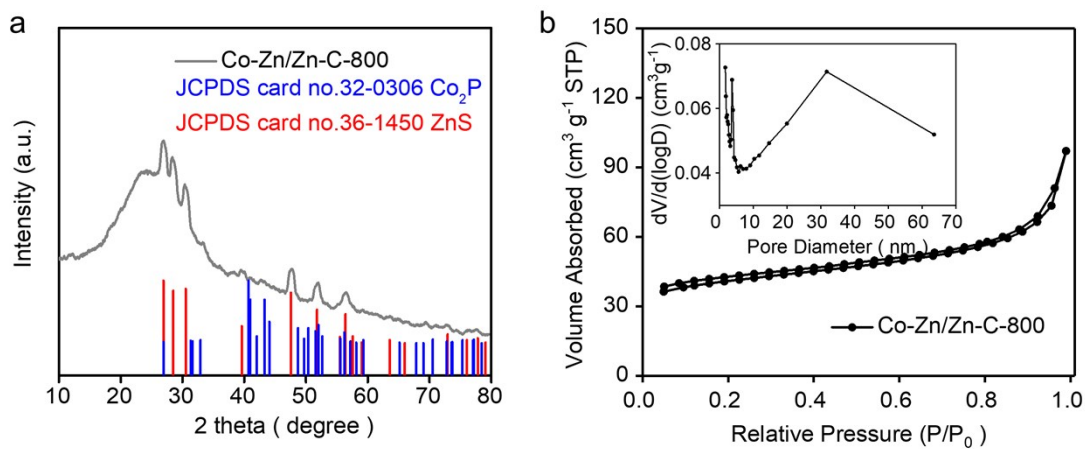


Fig. S2 (a) XRD pattern and (b) N_2 adsorption-desorption isotherm of the Co-Zn/Zn-C-800. The inset is the pore size distribution.

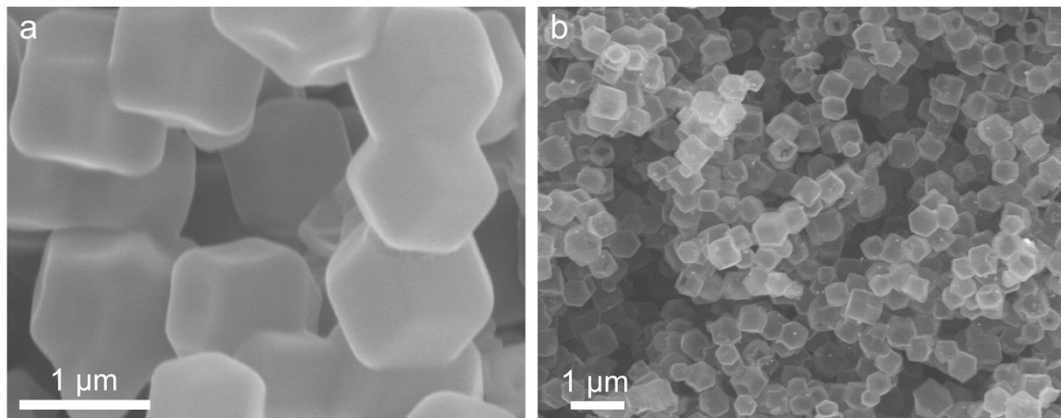


Fig. S3 SEM images of (a) Co-Zn/Zn-C-700 and (b) Co-Zn/Zn-C-900.

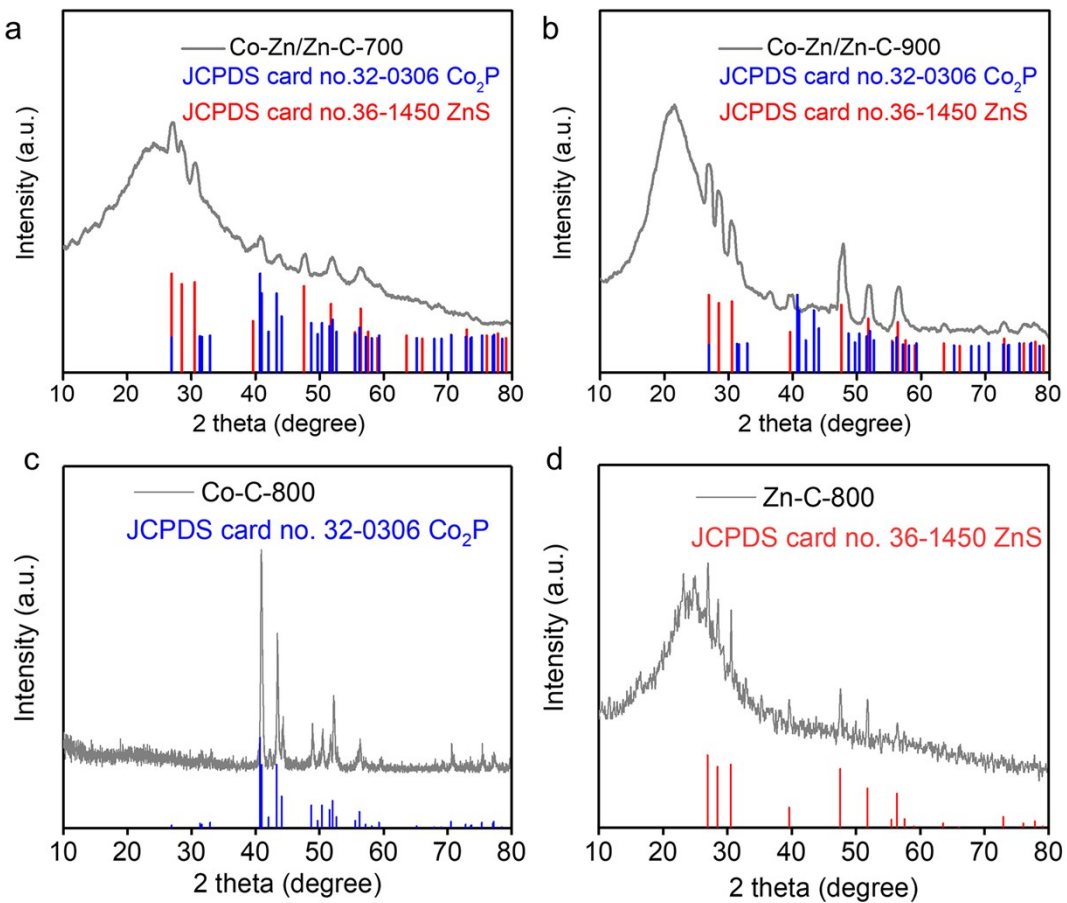


Fig. S4 XRD patterns of (a) Co-Zn/Zn-C-700, (b) Co-Zn/Zn-C-900, (c) Co-C-800 and (d) Zn-C-800.

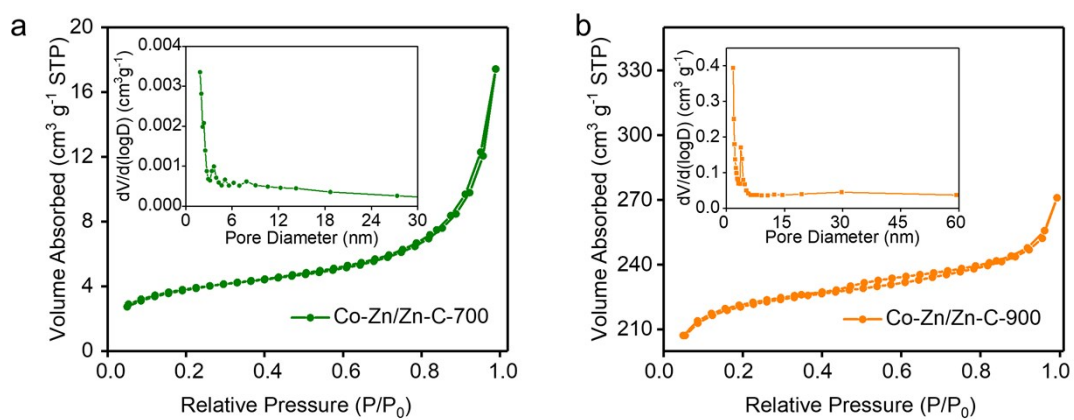


Fig. S5 N_2 adsorption-desorption isotherms of (a) Co-Zn/Zn-C-700 and (b) Co-Zn/Zn-C-900. The inset is pore size distribution.

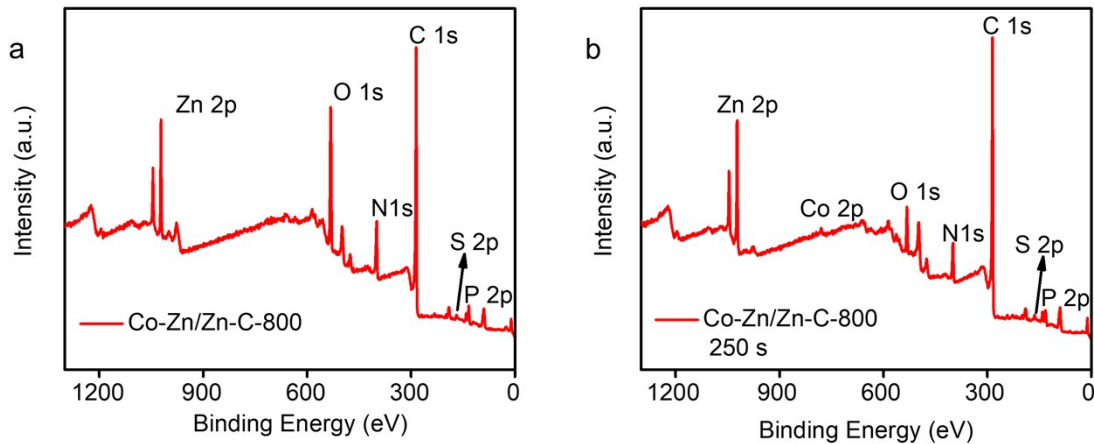


Fig. S6 Full XPS spectra of Co-Zn/Zn-C-800 (a) before (b) after 250 s etching.

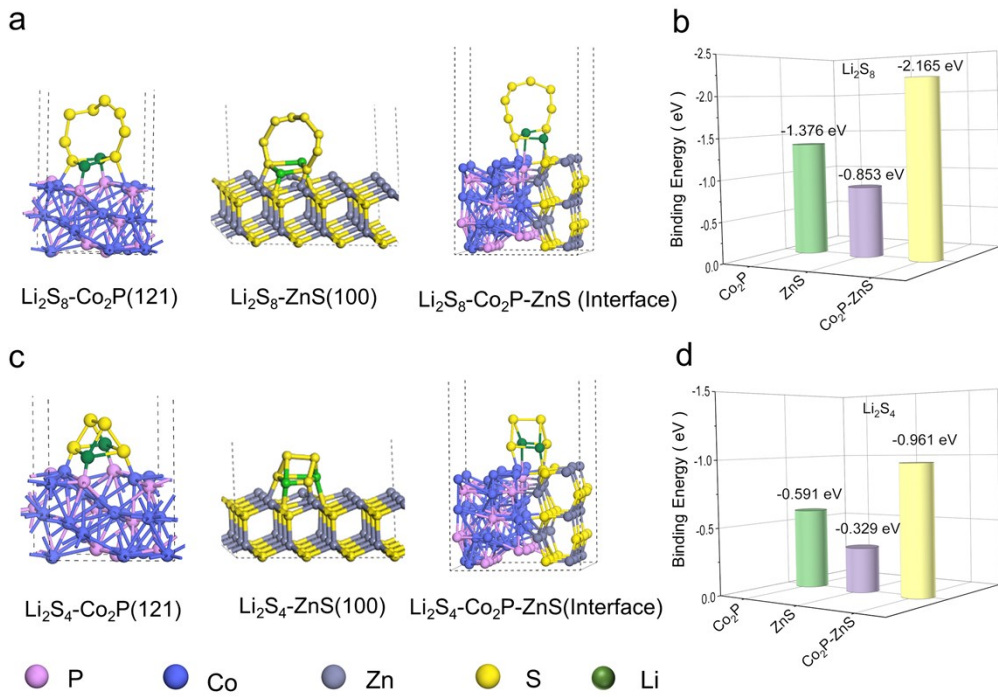


Fig. S7 (a and c) The stable adsorption configurations of Li_2S_n ($n = 8$ and 4) clusters on Co_2P (121) plane, ZnS (100) plane and $\text{Co}_2\text{P}-\text{ZnS}$ heterostructure interface, together with (b and d) the comparison of calculated adsorption energies. Pink, purple, gray, yellow and green balls represent P, Co, Zn, S and Li atoms, respectively.

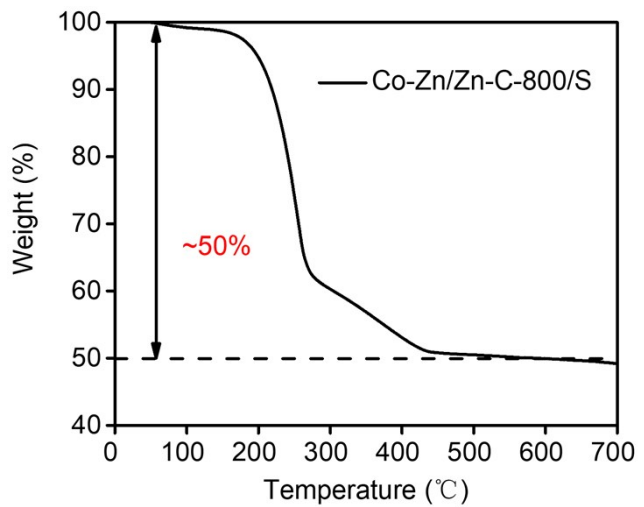


Fig. S8 TGA curve of Co-Zn/Zn-C-800/S achieved under N₂ atmosphere at heating rate of 10 °C min⁻¹.

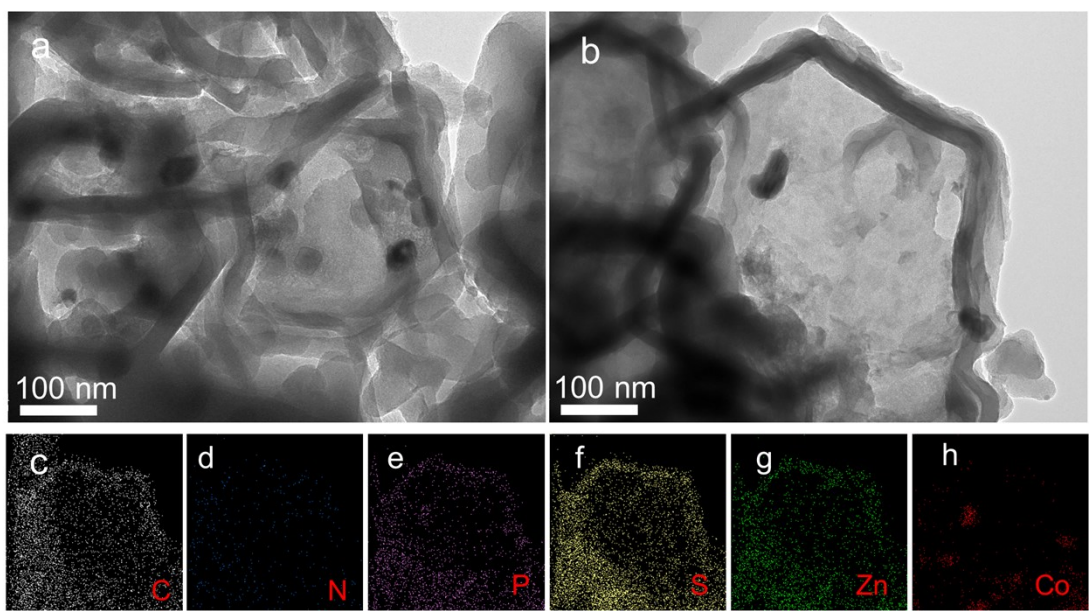


Fig. S9 (a) TEM image, (b) HRTEM image and the corresponding elemental mapping analysis of (c-h) of Co-Zn/Zn-C-800/S.

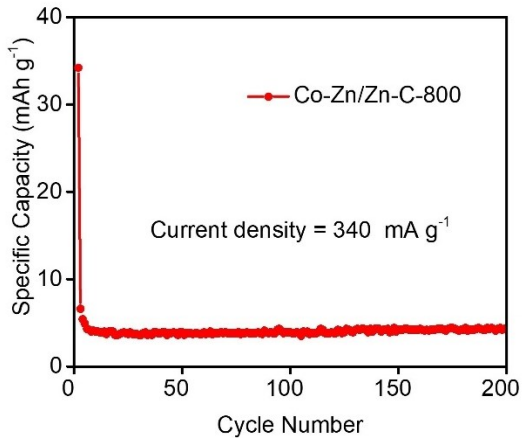


Fig. S10 Stability test of Co-Zn/Zn-C-800 | Li control cell at 340 mA g⁻¹.

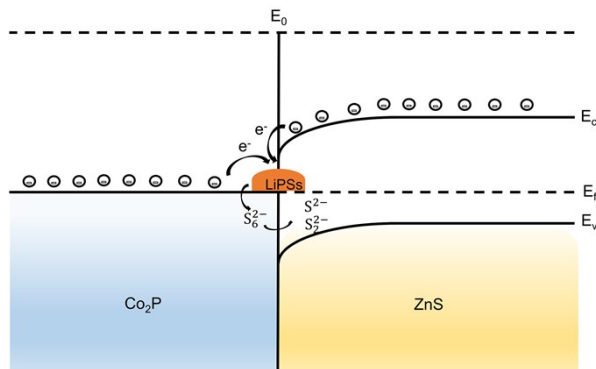


Fig. S11 Schematic illustration of the interface contact and the possible catalytic mechanism of Co_2P - ZnS heterostructure.

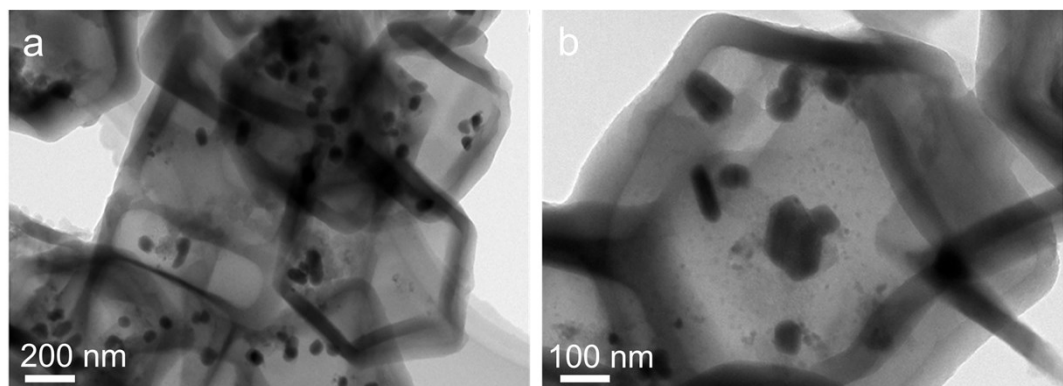


Fig. S12 TEM images of Co-Zn/Zn-C-800/S after 500 cycles at 1 C.

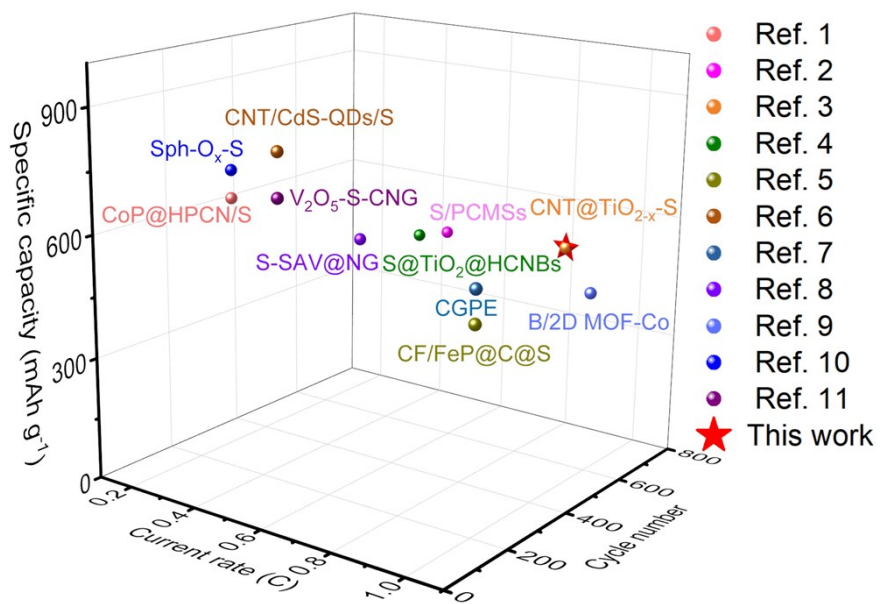


Fig. S13 Comparison of electrochemical performances among Co-Zn/Zn-C-800/S electrode and the literature reported sulfur cathodes.



Fig. S14 Optical image of blank Li_2S_6 solution and after adsorbing with Co-C-800 and Zn-C-800, respectively.

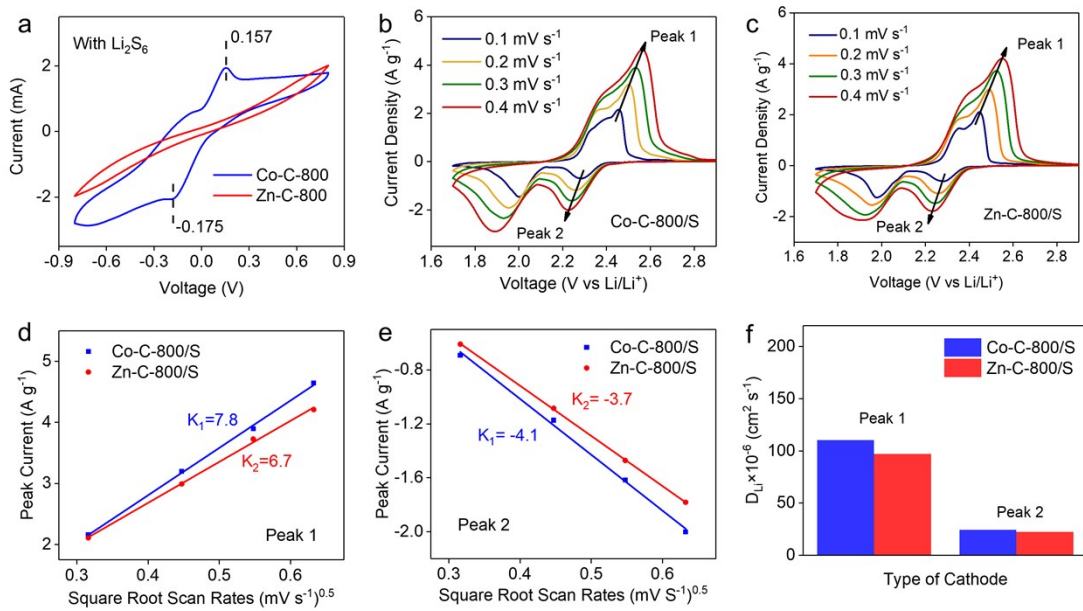


Fig. S15 (a) CV curves of Li_2S_6 symmetric cells from -0.8 to 0.8 V at 10 mV s^{-1} of Co-C-800 and Zn-C-800. (b and c) CV curves of different electrodes at various scanning rates; (d-f) The kinetic plots and diffusion coefficient (D_{Li^+}) of Li^+ ion corresponding peak 1 and 2 on Co-C-800/S and Zn-C-800/S cathodes.

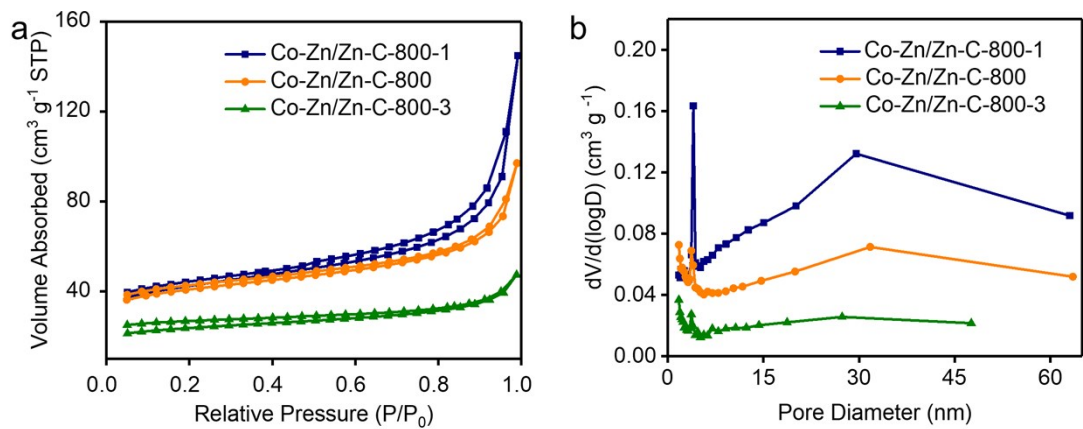


Fig. S16 (a) N_2 adsorption-desorption isotherms and (b) pore size distributions.

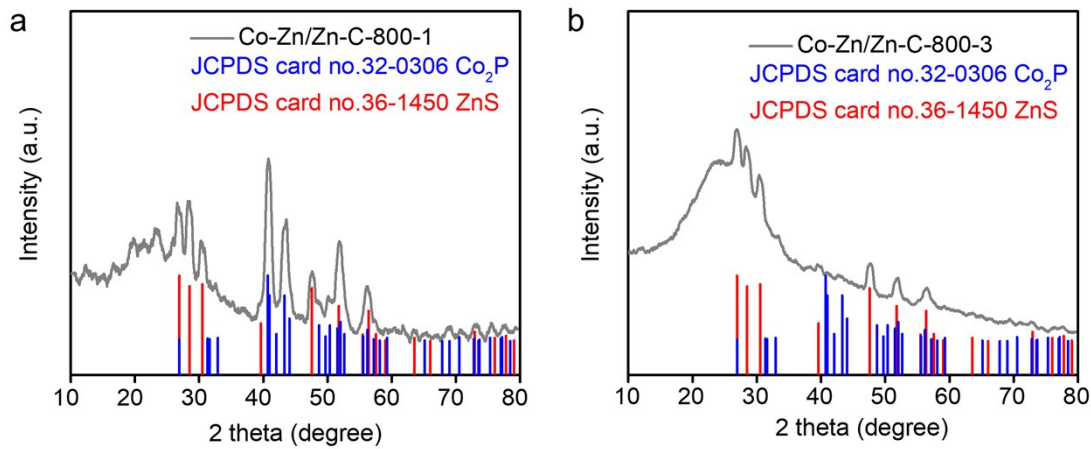


Fig. S17 XRD patterns of (a) Co-Zn/Zn-C-800-1 and (b) Co-Zn/Zn-C-800-3.

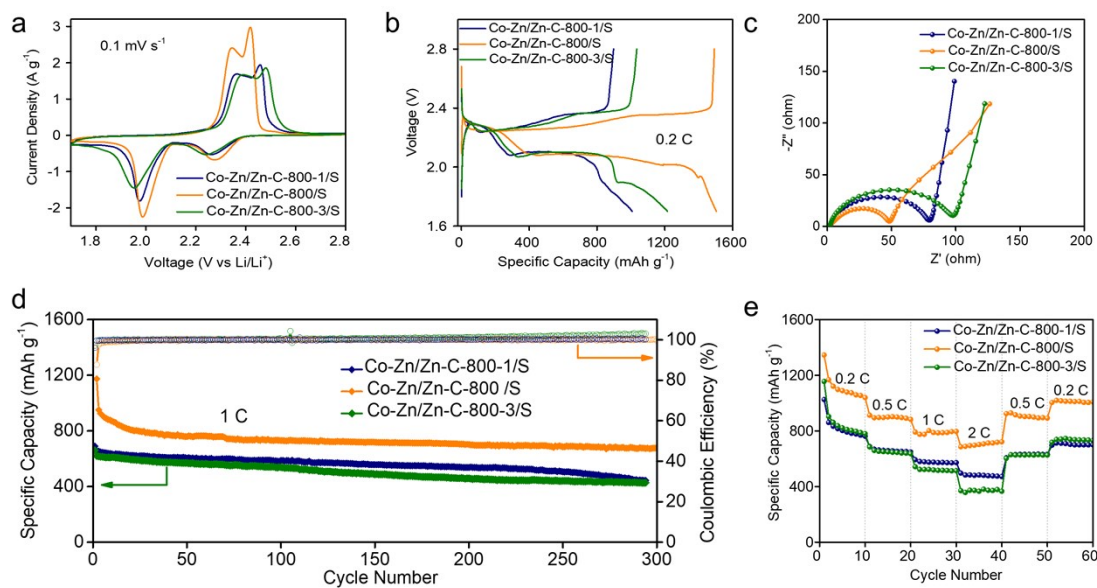


Fig. S18 (a) Galvanostatic charge–discharge curves, (b) CV curves, (c) EIS spectra, (d) cycling performance at 1 C, and (e) rate performance of different samples.

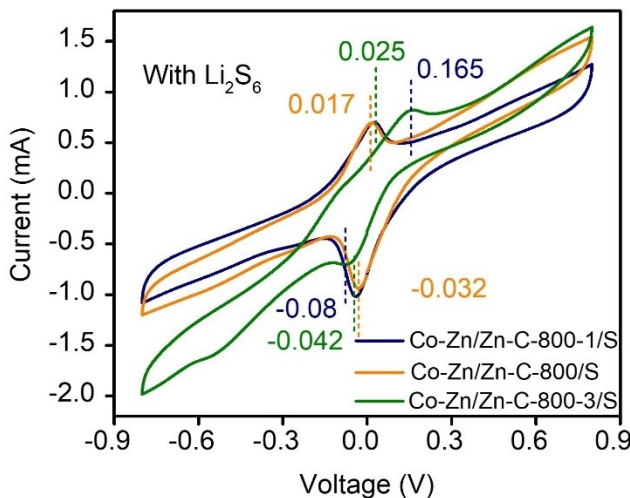


Fig. S19 CV curves of Li_2S_6 symmetric cells from -0.8 to 0.8 V at 10 mV s^{-1} .

Supporting References:

- 1 Z. Ye, Y. Jiang, J. Qian, W. Li, T. Feng, L. Li, F. Wu and R. Chen, *Nano Energy*, 2019, **64**, 103965.
- 2 S. Liu, T. Zhao, X. Tan, L. Guo, J. Wu, X. Kang, H. Wang, L. Sun and W. Chu, *Nano Energy*, 2019, **63**, 103894.
- 3 Y. Wang, R. Zhang, J. Chen, H. Wu, S. Lu, K. Wang, H. Li, C. J. Harris, K. Xi, R. V. Kumar and S. Ding, *Adv. Energy Mater.*, 2019, **9**, 1900953.
- 4 H. Gu, H. Wang, R. Zhang, T. Yao, T. Liu, J. Wang, X. Han and Y. Cheng, *Ind. Eng. Chem. Res.*, 2019, **58**, 18197-18204.
- 5 J. Shen, X. Xu, J. Liu, Z. Liu, F. Li, R. Hu, J. Liu, X. Hou, Y. Feng, Y. Yu and M. Zhu, *ACS Nano*, 2019, **13**, 8986-8996.
- 6 D. Cai, L. Wang, L. Li, Y. Zhang, J. Li, D. Chen, H. Tu and W. Han, *J. Mater. Chem. A*, 2019, **7**, 806-815.
- 7 D. Yang, L. He, Y. Liu, W. Yan, S. Liang, Y. Zhu, L. Fu, Y. Chen and Y. Wu,

- J. Mater. Chem. A*, 2019, **7**, 13679-13686.
- 8 G. Zhou, S. Zhao, T. Wang, S.-Z. Yang, B. Johannessen, H. Chen, C. Liu, Y. Ye, Y. Wu, Y. Peng, C. Liu, S. P. Jiang, Q. Zhang and Y. Cui, *Nano Lett.*, 2020, **20**, 1252-1261.
- 9 Y. Li, S. Lin, D. Wang, T. Gao, J. Song, P. Zhou, Z. Xu, Z. Yang, N. Xiao and S. Guo, *Adv. Mater.*, 2020, **32**, 1906722.
- 10 Y. Liu, Z. Ge, Z. Sun, Y. Zhang, C. Dong, M. Zhang, Z. Li and Y. Chen, *Nano Energy*, 2020, **67**, 104216.
- 11 C. Wang, Y. Yi, H. Li, P. Wu, M. Li, W. Jiang, Z. Chen, H. Li, W. Zhu and S. Dai, *Nano Energy*, 2020, **67**, 104253.